The Journal of Organic Chemistry

VOLUME 64, NUMBER 15 JULY 23, 1999

New Proton-Ionizable Lariat Ethers with Picrylamino-Type Side Arms and Their Alkali Metal Salts. Synthesis and Structural Studies[1]

Richard A. Bartsch,* Hong-Sik Hwang, Vladimir S. Talanov, Galina G. Talanova, and David W. Purkiss

Department of Chemistry and Biochemistry, Texas Tech University, Lubbock, Texas 79409-1061

Robin D. Rogers

Department of Chemistry, The University of Alabama, Tuscaloosa, Alabama 35487-0336

Received January 22, 1999

Twelve novel proton-ionizable dibenzo lariat ethers with picrylamino-type sidearms attached to the central carbon of a three-carbon bridge have been prepared in high yields by a three-step synthesis from the lariat ether alcohols via the corresponding lariat ether mesylates and amines. Structural studies conducted in solution by ^{1}H NMR spectroscopy and in the solid state by X-ray diffraction show that the picrylamino-type lariat ethers are preorganized for metal ion complexation with the sidearms oriented toward the macrocyclic polyether cavities due to intramolecular NH···O bonding. Structural investigations of the alkali metal salts of representative ionized picrylamino-lariat ethers in solution demonstrate cooperative coordination of the metal cation by the macrocyclic polyether unit and the ionized sidearm that serves as the counterion with the negative charge localized on the one of *o*-nitro groups. In the Li^+ salt of ionized *sym*-(picrylamino)-dibenzo-14-crown-4, this places the aromatic ring of the sidearm perpendicular to the plane of the four ring oxygens.

Introduction

Proton-ionizable lariat ethers with an ionizable group in a sidearm that is attached to the crown ether (CE) moiety provide highly selective ligands for the recognition and separation of alkali metal cations.[2] A special type of proton-ionizable lariat ethers that has attracted considerable attention during the past decade is the class of chromogenic ionophores[3] in which the ionizable group is part of the chromophore unit. Such ligands are potential photometric reagents for metal ion determination, since replacement of the chromophore group proton with a cation produces a color change. In particular, Takagi and co-workers[4] and later Bubnis, Pacey, and others[5] reported the synthesis of the proton-ionizable lariat ethers containing picrylamino-type chromophores in the sidearms (e.g., **1** and **2**). The efficiency and selectivity of alkali

(1) Presented in part at the 214th National Meeting of the American Chemical Society, Las Vegas, NV, September 7−11, 1997; I&EC 35 and 45.

(2) Gokel, G. W.; Schall, O. F. In *Comprehensive Supramolecular Chemistry*; Gokel, G. W., Ed.; Pergamon Press: New York, 1996; Vol. 1, pp 97−152.

(3) Hayashita, T.; Takagi, M. In *Comprehensive Supramolecular Chemistry*; Gokel, G. W., Ed.; Pergamon Press: New York, 1996; Vol. 1, pp 635−669.

(4) Takagi, M.; Nakamura, H.; Ueno, K. *Anal. Lett.* **1977**, *10*, 1115. Nakamura, H.; Takagi, M.; Ueno, K. *Anal. Chem.* **1980**, *52*, 1668. Katayama, Y.; Fukuda, R.; Takagi, M. *Anal. Chim. Acta* **1986**, *185*, 295.

(5) Pacey, G. E.; Bubnis, B. P. *Anal. Lett.* **1980**, *13 (A12)*, 1085. Pacey, G. E.; Wu, Y. P.; Bubnis, B. P. *Analyst* **1981**, *106*, 636. Bubnis, B. P.; Steger, J. L.; Wu, Y. P.; Meyers, L. A.; Pacey, G. E. *Anal. Chim. Acta* **1982**, *139*, 307. Bubnis, B. P.; Pacey, G. E. *Talanta* **1984**, *31*, 1149.

(6) Bartsch, R. A.; Liu, Y.; Kang, S. I.; Son, B.; Heo, G. S.; Hipes, P. G.; Bills, L. J. *J. Org. Chem.* **1983**, *48*, 4864. Walkowiak, W.; Charewicz, W. A.; Kang, S. I.; Yang, I.-W.; Pugia, M. J.; Bartsch, R. A. *Anal. Chem.* **1990**, *62*, 2018. Elshani, S.; Noriyuki, R.; Wai, C. M.; Natale, N. R.; Bartsch, R. A. *J. Heterocycl. Chem.* **1998**, *35*, 875.

10.1021/jo990116h CCC: $18.00
Published on Web 07/02/1999

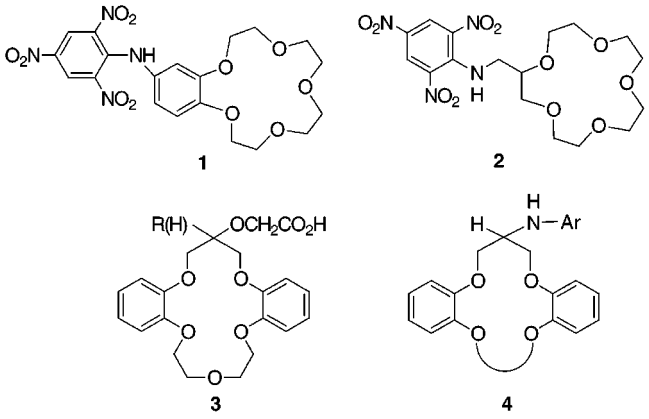

metal cation complexation by such reagents was found to vary with the ability of the pendent ionizable group to participate in metal ion coordination cooperatively with the CE moiety, as determined by the geometry of the sidearm attachment site.

In earlier work,[6] we developed proton-ionizable lariat ethers based upon a dibenzo-16-crown-5 platform (e.g., **3**) and related dibenzo-CEs in which a functional sidearm is attached to the central carbon atom of the three-carbon bridge via oxygen. In such lariat ethers, the sidearm may be oriented toward the CE cavity[7] so that the ligand is preorganized[8] for selective metal ion binding. We envisioned a series of new proton-ionizable dibenzo-CEs **4** with the sidearm attached to the CE framework by a nitrogen atom which possesses an acidic hydrogen. By analogy with **3**, the N-aryl sidearm in **4** might also favor preorganization of the lariat ether for metal ion complexation.

We now report a synthetic method for attachment of an amino group to the central carbon atom of dibenzo-14-crown-4 (DB14C4), dibenzo-16-crown-5 (DB16C5), and dibenzo-19-crown-6 (DB19C6) with subsequent conversion of these lariat ether primary amines into novel proton-ionizable lariat ethers containing picrylamino-type sidearms. To evaluate the potential preorganization of these compounds for metal ion coordination, structural studies were conducted in solution by ^{1}H NMR spectroscopy and in the solid state by X-ray diffraction. In addition, solution structures for several alkali metal salts of the ionized lariat ethers have been probed, with a particular emphasis on cooperation of the sidearm and macrocyclic unit in metal ion binding.

Results and Discussion

Synthesis. The synthetic route to *sym*-(amino)dibenzo-14-crown-4 (**5**), -16-crown-5 (**6**), and -19-crown-6 (**7**) is presented in Scheme 1. Precursor lariat ether alcohols **8**−**10**[9] were converted into lariat ether mesylates **11**−**13**, respectively, in 91−93% yields. The mesylates were reacted with NaN_3 and Cs_2CO_3 in DMF to produce lariat ether azides which, without isolation due to their potentially explosive nature, were reduced to the desired lariat ether amines **5**−**7** in 75−81% yields.

Reaction of lariat ether amines **5**−**7** with picryl chloride, 1-chloro-2,4-dinitro-6-trifluoromethylbenzene, 1-chloro-2,6-dinitro-4-trifluoromethylbenzene, or 1-chloro-4-

Scheme 1

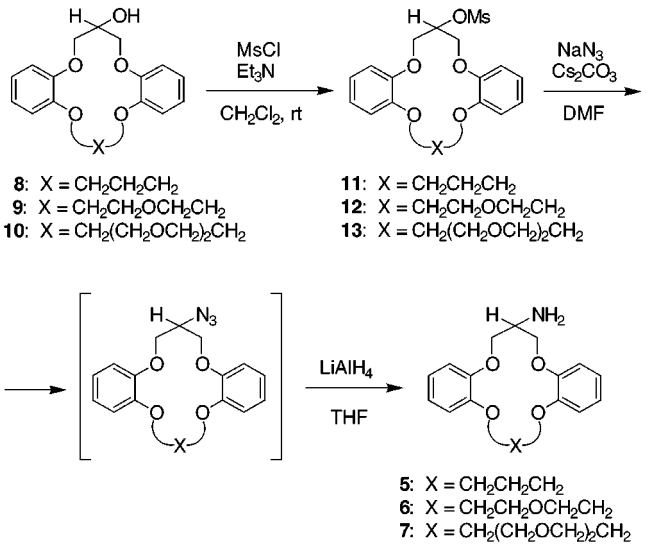

cyano-2,6-dinitrobenzene and $NaHCO_3$ in MeOH (Scheme 2) provided the new family of proton-ionizable lariat ethers **14**−**25**. Yields for the coupling reactions were high (88−96%), except for compounds **17** (68%) and **25** (61%).

Within this new family of proton-ionizable lariat ethers, there is a systematic structural variation of the crown ether ring size from DB14C4 to DB16C5 to DB19C6 for four different picrylamino-type sidearms. For a given ring size, there are four different sidearms in which the nature and arrangement of the electron-withdrawing substituents on the aromatic ring are changed. This variation is anticipated to influence the acidity of the proton-ionizable lariat ether and its spectral characteristics (particularly in the ionized form),[5] which may be important for future applications of these compounds in alkali metal cation recognition.

Structural Studies of the New Lariat Ethers and Their Alkali Metal Salts

Solid-State Structures of the Lariat Ethers. Suitable single crystals of proton-ionizable lariat ethers **17**−**19** were obtained, and their solid-state structures were determined by X-ray diffraction. This series contains compounds with different ring sizes of DB14C4 and DB16C5, as well as two different sidearms for a common DB16C5 ring. Computer drawings of the solid-state structures for compounds **17**−**19** are presented in Figures 1−3, respectively.

The three structures share a common feature. In each, the amino group of the sidearm donates a bifurcated hydrogen bond to an alkyl aryl ether oxygen atom of the polyether ring and to one oxygen atom of an *o*-nitro group in the aromatic ring of the sidearm. These intramolecular interactions position the sidearm N-aryl group over the crown ether cavity and thus preorganize the ligand for metal complexation by both the polyether oxygens and the *o*-nitro group. The H···O (crown ether) and H···O (nitro group) distances are similar in all three compounds and in the range of 2.21−2.28 and 1.89−2.21 Å, respectively. It is noted that the sidearm extends directly over the cavity for the DB16C5 macrocycles, but only the hydrogen-bonded nitro group resides over the cavity for the smaller DB14C4 ring.

The two DB16C5 macrocycles show an interesting difference in their conformations even though the only

(7) Bartsch R. A.; Kim, J. S.; Olsher, U.; Purkiss. D. M. *Supramol. Chem*. **1996**, *6*, 327.
(8) Cram, D. J. *Angew. Chem., Int. Ed. Engl.* **1986**, *25*, 1039.

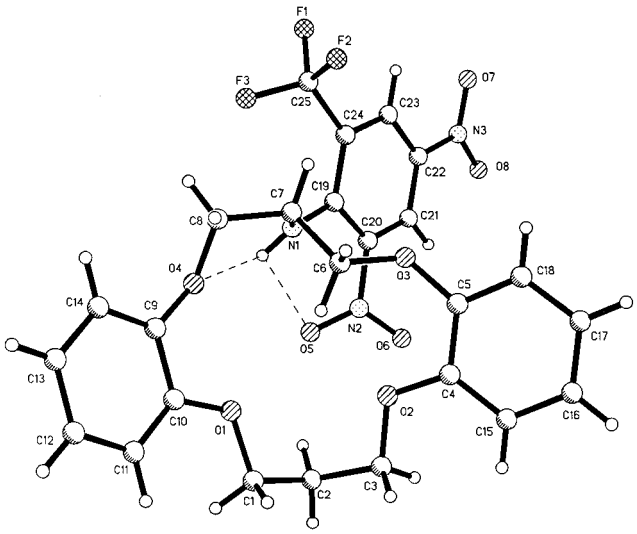

Figure 1. Solid-state structure of *sym*-(2,4-dinitro-6-trifluoromethylanilino)dibenzo-14-crown-4 (**17**).

Scheme 2

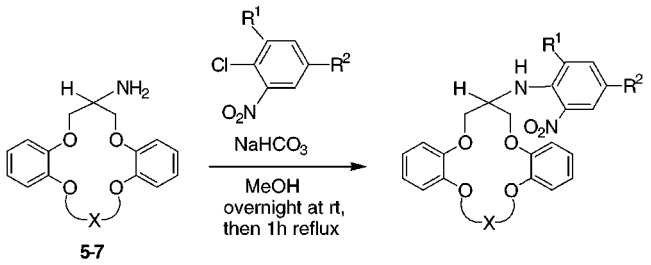

5-7

14: X = $CH_2CH_2CH_2$, $R^1 = NO_2$, $R^2 = NO_2$
15: X = $CH_2CH_2CH_2$, $R^1 = NO_2$, $R^2 = CN$
16: X = $CH_2CH_2CH_2$, $R^1 = NO_2$, $R^2 = CF_3$
17: X = $CH_2CH_2CH_2$, $R^1 = CF_3$, $R^2 = NO_2$
18: X = $CH_2CH_2OCH_2CH_2$, $R^1 = NO_2$, $R^2 = NO_2$
19: X = $CH_2CH_2OCH_2CH_2$, $R^1 = NO_2$, $R^2 = CN$
20: X = $CH_2CH_2OCH_2CH_2$, $R^1 = NO_2$, $R^2 = CF_3$
21: X = $CH_2CH_2OCH_2CH_2$, $R^1 = CF_3$, $R^2 = NO_2$
22: X = $CH_2(CH_2OCH_2)_2CH_2$, $R^1 = NO_2$, $R^2 = NO_2$
23: X = $CH_2(CH_2OCH_2)_2CH_2$, $R^1 = NO_2$, $R^2 = CN$
24: X = $CH_2(CH_2OCH_2)_2CH_2$, $R^1 = NO_2$, $R^2 = CF_3$
25: X = $CH_2(CH_2OCH_2)_2CH_2$, $R^1 = CF_3$, $R^2 = NO_2$

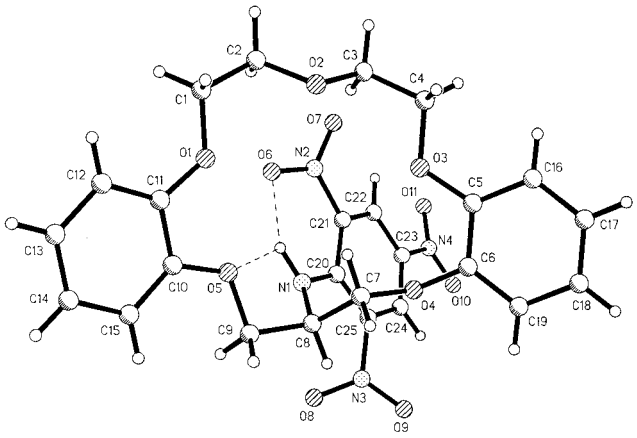

Figure 2. Solid-state structure of *sym*-(2,4,6-trinitroanilino)-dibenzo-16-crown-5 (**18**).

structural variation is the replacement of a *p*-cyano group in **19** with a *p*-nitro group in **18**. The conformational difference occurs in the O2−C3−C4−O3 ethylene linkage. In **19**, this group essentially forms a corner with three gauche torsion angles in a row (O2−C3, C3−C4, and C4−O3). In **18**, the more normal anti, gauche, anti conformation is observed. The reason for this difference is not readily apparent. However, a CH_2Cl_2 solvent molecule in the structure **18** appears to donate a weak C−H···O hydrogen bond to the *o*-nitro group which is directly over the crown cavity. This interaction is absent in **19**.

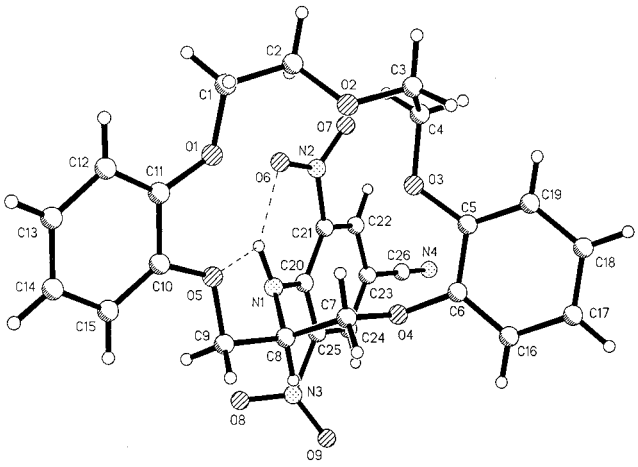

Figure 3. Solid-state structure of *sym*-(4-cyano-2,6-dinitroanilino)dibenzo-16-crown-5 (**19**).

The conformation of the propylene bridge is different in the DB14C4 and DB16C5 compounds. In the DB16C5 compounds **18** and **19**, the C6−O4, O4−C7, C7−C8, C8−C9, C9−O5, O5−C10 torsion angles have the conformation of gauche, anti, anti, −gauche, anti, anti. The corresponding torsion angles in the DB14C4 compound **17** (C4−O2−C3−C2−C1−O1−C10) are anti, anti, gauche, −gauche, anti, anti. In addition, the two torsion angles around O4 in **17** are distorted from the normal anti conformation to nearly 135° each. These structural features appear to make it more difficult to position the sidearm over the cavity in the DB14C4 compound.

Therefore in solid state, the lariat ethers are shown to exist in preorganized-for-metal-ion-binding conformations stabilized by intramolecular hydrogen bonding. However, the solid-state structure of a compound may vary significantly from that in solution, where solvation effects and conformational dynamics are important. Since the proton-ionizable lariat ethers **14**−**25** are intended for use as metal cation recognition agents in solvent extraction systems, their structures in organic solution must be considered as well, particularly in chloroform which is a commonly employed diluent for liquid−liquid extraction.

Solution Structures of the New Lariat Ethers. In solution, a lariat ether may adopt a number of different conformations, each of which is characterized by its own energy. The conformations coexist in a dynamic equilibrium, with their relative populations determined by their respective energies. Since the ^{1}H NMR spectra of **14**−**25** in $CDCl_3$ show only single sets of proton signals, fast conformational exchange on the NMR time scale is taking place in solutions of these compounds. Therefore, the observed spectra are attributed not to a definite lariat ether conformation, but to an average-weighted one[10a]

(9) Heo, G. S.; Bartsch, R. A.; Schlobohm, L. L.; Lee, J. G. *J. Org. Chem.* **1981**, *46*, 3574.

Table 1. ^{1}H NMR Data[a] for Selected Nuclei of Lariat Ethers 14−25

	δ (ppm)					$^3J_{1-2}$ (Hz)				
lariat ether	1-H	2-H_A	2-H_B	$\Delta\delta_{2A-B}$[b] (ppm)	$^2J_{2A-B}$ (Hz)	$^3J_{1-2A}$	$^3J_{1-2B}$	δ_{NH} (ppm)	$^3J_{1-NH}$ (Hz)	δ_{Pic} (ppm)
14	3.88	4.69	4.25	0.44	10.0	4.4	4.7	9.58 (d)	9.4	8.92 (s)
15	3.82	4.66	4.21	0.45	10.0	4.3	4.8	9.37 (d)	9.5	8.29 (s)
16	3.80	4.67	4.21	0.46	9.9	4.1	5.0	9.16 (d)	9.6	8.31 (s)
17	4.33	4.62	4.22	0.40	9.2	3.4	5.2	8.45 (br d)	9.0	9.02 (d),[c] 8.65 (d)
18	4.03	4.54	4.25	0.29	9.7	5.7	3.3	9.52 (d)	10.0	8.99 (s)
19	4.04	4.52	4.24	0.28	9.7	5.7	3.3	9.30 (d)	9.9	8.33 (s)
20	4.07	4.53	4.26	0.27	9.7	5.6	3.5	9.08 (d)	10.0	8.35 (s)
21	4.41	4.53	4.23	0.30	9.2	5.3	3.0	8.33 (br d)	7.8	8.99 (d),[d] 8.61 (d)
22	4.13	4.52	4.32	0.20	10.3	5.2	4.0	9.66 (d)	10.0	8.97 (s)
23	4.04	4.49	4.31	0.18	10.3	5.3	4.0	9.44 (d)	9.9	8.33 (s)
24	3.98	4.48	4.34	0.14	10.3	5.0	4.2	9.19 (d)	10.0	8.34 (s)
25	*e*	*e*	*e*	*e*	*e*	*e*	*e*	8.03 (br s)	*f*	8.98 (d),[g] 8.61 (d)

[a] In $CDCl_3$. [b] Calculated as $\Delta\delta_{A-B} = \delta_A - \delta_B$. [c] $^4J = 2.8$ Hz. [d] $^4J = 2.6$ Hz. [e] This region could not be analyzed due to the intermediate rate of exchange at 297 K. [f] Could not be determined. [g] $^4J = 2.7$ Hz.

which results from averaging of all lariat ether conformations present in solution with respect to their populations.

The structural investigation performed for compounds **14**−**25** by ^{1}H NMR spectroscopy focused primarily on the determination of the sidearm position relative to the CE moiety. Accordingly, signals from protons in the sidearm and the adjacent portion of the macrocycle were analyzed precisely. In $CDCl_3$ solution, the CE moieties of **14**−**25** possess symmetrical structures in which there is no differentiation of the signals for the 2 and 2′ protons and the 7 and 7′ protons (Figure 4), as well as protons in other matching positions on the two sides of the macroring. Nevertheless, the diastereotopic nonequivalence for pairs of protons on carbon atoms 2 and 2′ caused by the presence of a prochiral center (i.e., the 1-C atom) is well-defined as a difference of their chemical shift values, $\Delta\delta$. Although some nonequivalence of diastereotopic hydrogen atoms in methylene groups remote from the sidearm attachment site is also noticeable, their $\Delta\delta$ values could not be determined in the 300 MHz ^{1}H NMR spectra.

The spectral data for selected nuclei of lariat ethers **14**−**25** are presented in Table 1. Signal assignments for 2-H_A and 2-H_B (Figure 4) were verified by NOESY spectra as having or not having, respectively, cross-peaks with the proton signals for the N-aryl group.

As is readily evident from the data in Table 1, the difference in the chemical shift values for 2-H_A and 2-H_B ($\Delta\delta_{2A-B}$) varies with the structure of the -X- unit (Figure 4), rather than that of the N-aryl group, decreasing as the macrocycle size is expanded from 14 to 16 to 19 members. Therefore, the bridgehead geometry and, correspondingly, the sidearm orientation in the lariat ether is affected by the structure of the CE moiety, even the remote −X− unit.

The geometry of the sidearm attachment site may be assessed from the coupling constants of 1-H with 2-H_A and 2-H_B ($^3J_{1-2A}$ and $^3J_{1-2B}$, respectively), since these are determined by the magnitude of the corresponding dihedral angles, ϕ^1 and ϕ^2, between the coupled atoms (Figure 5a). According to the Karplus equation,[10b] for dihedral angles from 0 to 90°, a larger angle decreases the J value. As is evident from the data in Table 1, the coupling constants for the 1-H−2-H_A protons of the 14-membered lariat ethers **14**−**17** are smaller than those for the 1-H−2-H_B protons. Hence for **14**−**17**, $\phi^1 > \phi^2$. In

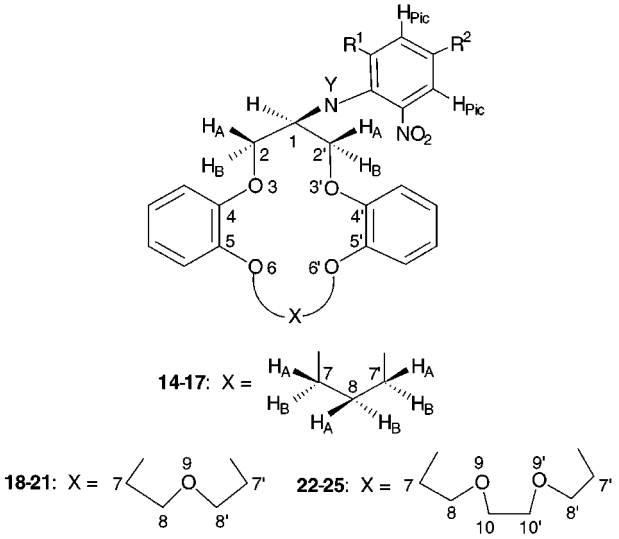

Figure 4. Atom numbering scheme for the ^{1}H NMR studies of lariat ethers **14**−**25** (Y = H) and their alkali metal salts (Y = Li, Na or K). (Methylene group protons are given the numbers of the corresponding carbon atoms.)

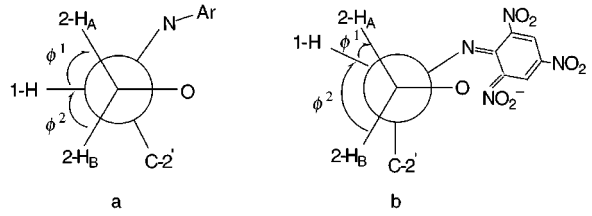

Figure 5. Newman projections of (a) the lariat ethers and (b) the alkali metal salts of ionized **14** along the 2-C−1-C bond.

contrast, for the 16- and 19-membered lariat ethers, $^3J_{1-2A} > {}^3J_{1-2B}$ and, correspondingly, $\phi^1 < \phi^2$. Therefore, in the averaged conformation, the N-aryl group of the DB16C5 and DB19C6 compounds is more oriented toward the CE moiety than it is in the corresponding DB14C4 compounds. Accordingly, the distance between 2-H_A and the amino-group nitrogen increases as the macrocyclic polyether ring is expanded. Therefore, the sidearm effect on the chemical shift of 2-H_A diminishes as the size of the macrocycle increases and the $\Delta\delta_{2A-B}$ value decreases for the change from 14- to 16- to 19-membered lariat ethers, as mentioned above (Table 1). Also, it is important to note the correlation between the sidearm position and the $\Delta\delta_{2A-B}$ value. The more the sidearm is oriented toward the CE moiety, the smaller

(10) Günther, H. *NMR Spectroscopy: Basic Principles, Concepts, and Applications in Chemistry*; Wiley: New York, 1995; (a) Chapter 9, (b) Chapter 4.

is the observed $\Delta\delta_{2A-B}$ value. This feature will be used again in discussion of solution structures of alkali metal salts of the ionized lariat ethers (vide infra).

In the solid-state structures of lariat ethers **17**−**19** (Figures 1−3, respectively), the sidearms are oriented toward the macrocyclic cavity due to intramolecular hydrogen bonding of the NH proton with one of the endocyclic oxygen atoms. This factor may also favor preorganized lariat ether conformations in solution as well. The degree of sidearm orientation toward the macrocyclic cavity in the averaged lariat ether conformation in solution should increase as the population of conformations involving intramolecular hydrogen bonding is enhanced. Therefore, the probability of NH···O bond formation in the DB14C4 compounds **14**−**17** is expected to be lower than in the DB16C5 and DB19C6 analogues.

Since the amino groups in **14**−**25** are attached directly to the macrocyclic polyether units, they are likely to form hydrogen bonds with the nearest oxygen atom (3-O or 3′-O) in solution, as found in the solid-state structures of **17**−**19**. This supposition is consistent with the undefinably small diastereotopic nonequivalence of protons in the −X− units (vide supra). At the same time, symmetry is evident in the NMR spectra for the CE moieties of **14**−**25**. Therefore, no fixed NH···O bond with a particular endocyclic oxygen atom is observed for these compounds in solution, unlike in solid state. Instead, two equally populated sets of the lariat ether conformations in which the amino-group proton binds with either the 3-O or 3′-O endo-cyclic atom must be present in solution.

The NH proton signals for the N-(2,4-dinitro-6-trifluoromethylphenyl)-substituted lariat ethers **17**, **21**, and **25** have distinctive positions and shapes (Table 1). The observed broadness of these signals for compounds which contain only one *o*-nitro group indicates that the exchange process involving the NH proton is slower than that for a lariat ether with two *o*-nitro groups on the aromatic ring of the sidearm. This effect of the number of *o*-nitro groups on the exchange rate for the NH proton provides evidence of *o*-nitro group participation in hydrogen bonding with this proton in solution. Thus, the structures in solution are consistent with the solid-state structures (Figures 1−3) which have bifurcated intramolecular NH···O bonds involving oxygens of both the macrocycle and an *o*-nitro group of the sidearm.

Thus, the ^{1}H NMR spectral studies reveal an averaged conformation in solution in which the sidearm is oriented toward the macrocyclic polyether cavity which preorganizes the lariat ether for cation complexation.

Solution Structures of Alkali Metal Salts of the Ionized Lariat Ethers. To probe for cooperative interactions of the macrocyclic polyether unit and ionized sidearm with a complexed metal ion in solution, alkali metal salts of the ionized lariat ethers were examined by ^{1}H NMR spectroscopy in $CDCl_3$. Reactions of lariat ethers **14**, **18**, and **22**, which have the same picrylamino sidearm but different-sized CE units, with the appropriate metal hydride in THF gave the corresponding lariat ether Li^+, Na^+, and K^+ amides (Figure 4). The reactions were accompanied by a color change of the solution from yellow to blood red which demonstrates the chromogenic behavior of these compounds upon ionization. Metal salt formation also produced dramatic changes in the ^{1}H NMR spectra of the lariat ethers (Figure 6). Absence of

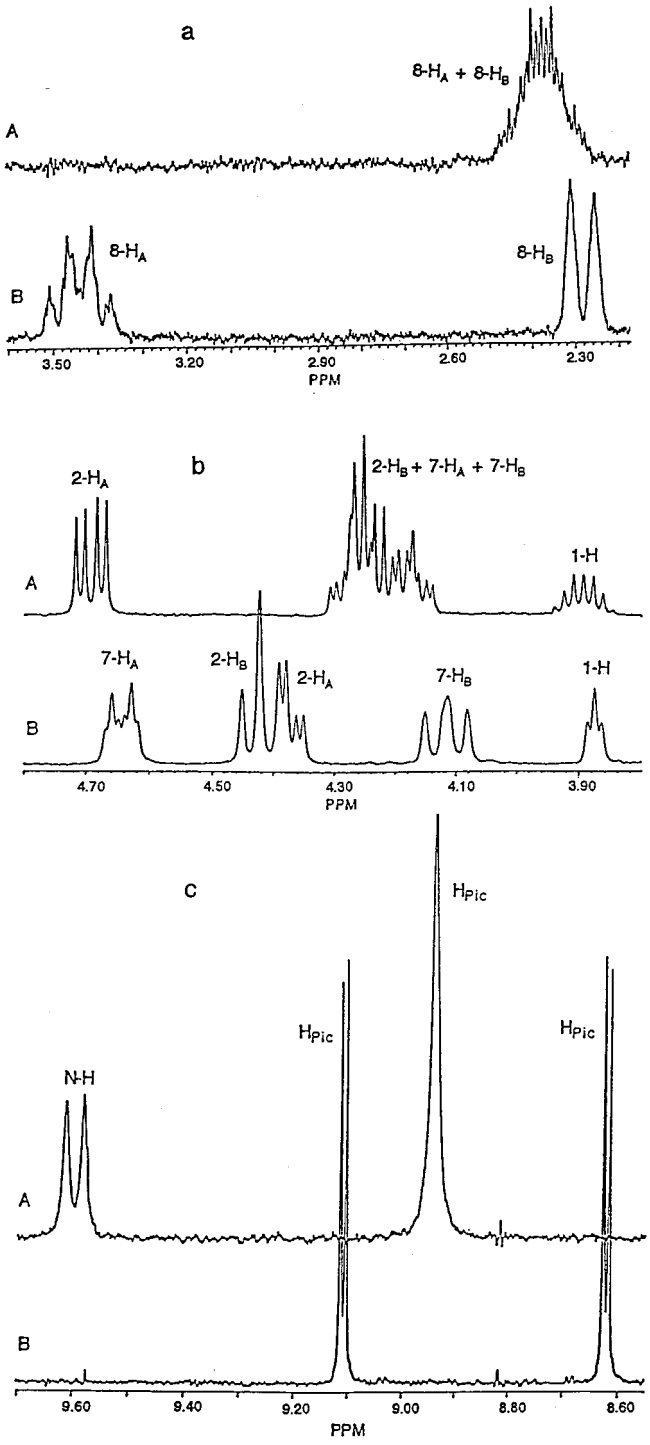

Figure 6. ^{1}H NMR spectra ($CDCl_3$) of **14** (A) and its Li^+ salt (B) in the regions for (a) 8-H, (b) 1-H, 2-H, and 7-H, and (c) the sidearm protons.

a doublet for the NH group in the spectra of the salts verified complete proton replacement by the alkali metal cation.

Since lariat ether **14** with the smallest ring size provided the simplest NMR spectrum, its alkali metal picrylamides were investigated in greater detail. Characteristics of the ^{1}H NMR spectra in the aliphatic proton region for the alkali metal salts of ionized **14** including the calculated values of the chemical shift nonequivalence ($\Delta\delta$) for the diastereotopic protons on the 2-, 7-, and 8-C atoms (Figure 4) are presented in Table 2. It should be

Table 2. ^{1}H NMR Data[a] for Selected Nuclei of Lariat Ether 14 and Alkali Metal Salts of the Ionized 14

	δ (ppm)					$^3J_{1-2}$ (Hz)		δ (ppm)			δ (ppm)		
Y[b]	1-H	2-H_A	2-H_B	$\Delta\delta_{2A-B}$[c] (ppm)	J_{2A-B} (Hz)	$^3J_{1-2A}$	$^3J_{1-2B}$	7-H_A	7-H_B	$\Delta\delta_{7A-B}$[c] (ppm)	8-H_A	8-H_B	$\Delta\delta_{8A-B}$[c] (ppm)
H	3.88	4.69 (dd)	4.25 (dd)	0.44	10.0	4.4	4.7	4.22 (m)		*d*	2.37 (m)		*d*
Li	3.88	4.37 (dd)	4.43 (d)	0.06	8.3	3.4	0	4.66	4.11	0.55	3.44	2.28	1.16
Na	3.84	4.51 (dd)	4.22 (d)	0.29	9.0	3.2	0	4.44	3.94	0.50	2.53	2.14	0.39
K	3.71	4.45[e]	4.03 (d)	0.42	9.3	*d*	0	4.49	3.87	0.62	2.44	2.21	0.23

[a] In $CDCl_3$. [b] See Figure 4. [c] $\Delta\delta_{A-B} = \delta_A - \delta_B$. [d] Could not be determined. [e] The signal multiplicity could not be determined due to overlap with the signal for 7-H_A.

noted that in the spectra of the alkali metal salts of ionized **14**, as well as in the spectrum of the parent ligand, no differences were observed for the signals of protons on the symmetrically situated carbons, 2-C and 2′-C or 7-C and 7′-C. As can be seen from the data in Table 2, each of the salts has a distinctive spectrum and, therefore, geometry of the complex.

Information about the orientation of the sidearm in the ionized lariat ether−alkali metal cation complexes was obtained by analysis of the coupling constants for 1-H with 2-H_A and 2-H_B. In contrast with the spectrum for **14**, $^3J_{1-2B} = 0$ in its Li^+, Na^+, and K^+ amide salts. In accordance with the Karplus equation,[10b] this establishes a dihedral angle ϕ^2 in the salts of 80−90° (Figure 5b) which results from greater orientation of the sidearm toward the CE cavity in comparison with that in the parent ligand **14**. This is consistent with joint participation of the sidearm and the macrocyclic polyether unit in metal ion coordination for all of the alkali metal salts of ionized **14**.

In the spectra of the alkali metal salts of ionized **14**, signals for the diastereotopic protons on the 2-C, 7-C, and 8-C atoms undergo dramatic changes relative to those for the parent ligand **14** (Table 2, Figure 6a,b). The diastereotopic nonequivalency, $\Delta\delta$, for these sets of protons is caused by the metal cation (if its location is unsymmetrical relative to the plane formed by the CE oxygens) and/or the sidearm. Analysis of changes in the magnitude of $\Delta\delta$ with metal ion variation provides further insight into the geometry of the complexes in solution. The positioning of Li^+, Na^+, or K^+ relative to the CE cavity should vary in accordance with the cation-to-macrocycle size fit.[11] Within the series of alkali metal ions, only the size of Li^+ matches the macrocyclic cavity of this DB14C4 lariat ether. However, it has been shown that in the solid-state Li^+ is positioned slightly above the plane of the four ring oxygens in a DB14C4 lariat ether carboxylate salt.[12] Since Na^+ and K^+ are too large to fit within a DB14C4 cavity, they must form perching complexes. Accordingly, the metal ion influence upon the $\Delta\delta$ value should increase:[13] $Li^+ < Na^+ < K^+$. On the other hand, the influence of the sidearm upon $\Delta\delta$ will be restricted to neighboring atoms. An effect on the protons of the transannular 7-C and 8-C atoms will be seen only if the sidearm is situated close to these atoms. In that case, its effect on the $\Delta\delta_{2A-B}$ will be diminished (see Figure 5 and the earlier discussion for neutral ligands).

The much larger $\Delta\delta_{8A-B}$ value for the Li^+ salt of **14** (1.16 ppm) than for the Na^+ and K^+ salts is noteworthy. Since the $\Delta\delta_{8A-B}$ values vary inversely with the size of metal ions and taking into account the arguments presented above, it is concluded that the sidearm position, not the metal ion, makes the major contribution to $\Delta\delta_{8A-B}$. Thus, the large $\Delta\delta_{8A-B}$ value for the Li^+ amide of **14** results from proximity of the sidearm to the 8 position of the macrocycle, particularly to 8-H_A. In the complex, the sidearm reaches over small Li^+ to approach the 8-H_A atom. The much smaller $\Delta\delta_{8A-B}$ values observed for the Na^+ and K^+ salts of ionized **14** (0.39 and 0.23 ppm, respectively) show a markedly diminished influence of the sidearm on 8-H_A. This is consistent with both Na^+ and K^+ perching on the four CE oxygens in their complexes, but the sidearm is now too short to effectively approach the 8 position by reaching over these larger metal ions. The somewhat larger value of $\Delta\delta_{8A-B}$ for the Na^+ complex than that for K^+ complex provides additional evidence for sidearm participation in cation coordination.

The observed diastereotopic nonequivalence of 2-H_A and 2-H_B increases in the order $Li^+ < Na^+ < K^+$ which shows that the effect of the metal ion and the N-aryl group on the $\Delta\delta_{2A-B}$ increases in this series. Therefore, we can presume that the distances of both the metal ion and the sidearm to the CE plane increase in the same order. Thus, the variation in $\Delta\delta_{2A-B}$ for ionized **14** with the change of the metal ion further supports the proposed solution structures of the complexes.

In contrast, the $\Delta\delta$ value for diastereotopic 7-H_A and 7-H_B is almost unaffected by metal ion variation. Presumably for this pair of protons, the two opposing trends as the size of the metal ion increases (i.e., an increase in $\Delta\delta_{7A-B}$ due to an enhanced influence of the perching metal ion and a decrease in $\Delta\delta_{7A-B}$ because of a greater distance between the ionized sidearm and the 7-C atom) compensate each other.

Thus, this structural analysis of the alkali metal amides of **14** based upon the $\Delta\delta$ changes in their ^{1}H NMR spectra provides strong evidence for cooperative metal ion coordination by the macrocyclic polyether unit and the ionized sidearm.

Changes in the aromatic region of the ^{1}H NMR spectrum for lariat ether **14** upon salt formation provide additional insight into the solution structures of the resultant complexes. Protons of the picryl moiety are equivalent in the neutral ligand **14**, but are nonequivalent in its alkali metal amides (Table 3, Figure 6c). The difference in chemical shifts for the two picryl protons demonstrates nonequivalency of the two nitro groups in the *o*-positions of the N-aryl group. This suggests that the negative charge in the ionized sidearm is localized

(11) Pedersen, C. J.; Frensdorff, H. K. *Angew. Chem., Int. Ed. Engl.* **1972**, *84*, 16. Poonia, N. S. *J. Am. Chem. Soc.* **1974**, *96*, 1012.

(12) Shoham, G.; Christianson, D. W.; Bartsch, R. A.; Heo, G. S.; Olsher, U.; Lipscomb, W. N. *J. Am. Chem. Soc.* **1984**, *106*, 1280.

(13) Positioning of a cation the same distance from H_A and H_B will produce the same effect on the chemical shifts of both protons. This will not induce any difference in chemical shifts for those protons. In perching complexes, the distances from the cation to H_A and H_B are different and so are their chemical shifts. Since Li^+ is expected to be only slightly above the macrocyclic plane, the effect of its position on the induced $\Delta\delta$ value will be the smallest. The cation radius increases $Li^+ < Na^+ < K^+$. A larger cation causes a greater desymmetrization in the complex and, therefore, a larger $\Delta\delta$ value.

Table 3. Chemical Shifts (ppm) and $\Delta\delta^a$ Values (ppm) for the Picryl Group Protons of 14, 18, and 22 and Alkali Metal Salts of the Ionized Lariat Ethers[b]

	14		18		22	
Y[c]	δ_{Pic}	$\Delta\delta_{Pic}$	δ_{Pic}	$\Delta\delta_{Pic}$	δ_{Pic}	$\Delta\delta_{Pic}$
H	8.94	0	8.99	0	8.97	0
Li	9.10, 8.61	0.49	9.06, 8.60	0.46	8.86, 8.28	0.58
Na	8.64, 8.60	0.04	8.95, 8.68	0.27	9.01, 8.72	0.29
K	8.60, 8.54	0.06	8.74, 8.69	0.05	8.73, 8.70	0.03

[a] The difference in chemical shift values for the two picryl protons. [b] In $CDCl_3$. [c] See Figure 4.

predominantly on one *o*-nitro group, which is oriented toward the CE-complexed metal ion and serves as the counterion. The picryl proton signals in the spectra of the Li^+ (Figure 6c) and Na^+ complexes of ionized **14** are sharp and well-resolved which indicates slow exchange of the two *o*-nitro groups on the NMR time scale. In contrast, the picryl proton signals of the K^+ salt are somewhat broader which suggests a faster exchange and hence, a shorter lifetime of the sidearm in a specific position in the complex. However, there is no differentiation of the signals for the 2 and 2′ protons or other protons in matching positions on the macroring. For the Li^+ salt of ionized **14**, $\Delta\delta_{8A-B}$ is much larger than $\Delta\delta_{7A-B}$ (Table 2). This indicates that the N-aryl group lies on a plane of symmetry passing through the 1-C and 8-C atoms and bisecting the DB14C4 macrocycle. Thus, the picryl group in the sidearm is perpendicular to the plane of the four CE oxygens.

The $\Delta\delta_{Pic}$ values for the picryl protons in the alkali metal salts of ionized **14** vary with the cation identity: $Li^+ \gg Na^+, K^+$. This trend further supports the proposed closer proximity of the ionized sidearm and the CE unit in the Li^+ complex of ionized **14** than in the Na^+ and K^+ complexes. When the distance between the N-aryl group of the sidearm and the CE moiety is small, the benzo groups of the CE deshield the inward-facing picryl proton to a much greater extent than the outward-facing one.[14]

Analysis of the ^{1}H NMR spectra for the alkali metal salts of ionized DB16C5 and DB19C6 lariat ethers **18** and **22**, respectively, in the region of 3.7−4.7 ppm was hampered by overlap with signals arising from the increased number of oxymethylene groups in these larger macrocycles. However, the changes observed in the aromatic regions of the spectra for **18** and **22** upon the salt formation (Table 3) demonstrate participation of both the ionized sidearm and the CE unit in metal ion complexation. The picryl proton nonequivalence, which is absent in the spectra of the lariat ethers themselves, is clearly evident in the alkali metal amide complexes of **18** and **23**. Since the magnitude of this nonequivalence, $\Delta\delta_{Pic}$, is taken as an indication of the distance between the sidearm and the CE benzo rings, analysis of its change with cation variation provides further information regarding the solution structures of the complexes. The $\Delta\delta_{Pic}$ values for the alkali metal salts of both ionized **18** and **22** decrease as the cation size is increased (Table 3), consistent with the results for the corresponding salts of the ionized **14**. The very small $\Delta\delta_{Pic}$ values of 0.03−0.06 ppm noted for the Na^+ and K^+ amides of **14** and the K^+ amides of **18** and **22** indicate that in these complexes the sidearm N-aryl group does not approach closely to the benzo groups of the CE.

These observations underscore an important role of the sidearm in the structural arrangement of the alkali metal salts of the ionized lariat ethers. The solution structures for the alkali metal salts of the picrylamino-type lariat ethers are shown to vary considerably as the metal ion is changed which suggests that stability of the complexes may differ as well. Results from extensive studies of metal ion recognition by these new chromogenic, proton-ionizable lariat ethers will be reported elsewhere.

(14) Although the nonequivalence of the sidearm aryl protons originates from the nonequivalence of the *o*-nitro groups, the $\Delta\delta_{Pic}$ value depends on both the electronic and magnetic environments of the protons. The electronic environments of the nonequivalent picryl protons will be nearly the same, since the distances between each of the picryl protons and the nonequivalent *o*-nitro groups are the same for all of the salts. Also, the distances between each of the picryl protons and the cation will vary only slightly as the metal ion is changed. Different magnetic environments arise from the differing spatial locations of the nonequivalent picryl protons relative to the benzo groups of the CE moiety, and become significant *only* for close proximity to these benzo groups.

Conclusions

Twelve new proton-ionizable lariat ethers (derivatives of *sym*-dibenzo-14-crown-4, *sym*-dibenzo-16-crown-5, and *sym*-dibenzo-19-crown-6) with picrylamino-type sidearms have been synthesized. Examination of the solid-state and solution structures of the compounds shows that they exist in the preorganized-for-metal-ion-binding conformations with the sidearm oriented toward the CE cavity and stabilized by intramolecular NH···O bonding. For alkali metal salts of the ionized lariat ethers in solution, cooperative metal ion coordination by the sidearm and the macrocyclic polyether unit is demonstrated.

Experimental Section

General Methods and Instrumentation. Melting points are uncorrected. FT-IR spectra were obtained for deposits from CH_2Cl_2 solutions onto NaCl plates. The ^{1}H NMR spectra were recorded at 300.133 MHz and chemical shifts (δ) are reported downfield from the internal standard, TMS. NOESY experiments were performed with the standard program and a mixing time of 0.20 s. Elemental analyses were performed by Desert Analytics Laboratory (Tucson, Arizona).

Materials. Unless otherwise specified, reagent-grade reactants and solvents were used as received from chemical suppliers. Lariat ether alcohols **8**−**10** were prepared by the literature method.[9] THF was freshly distilled from sodium metal ribbon and benzophenone ketyl. DMF was distilled from $MgSO_4$ under reduced pressure.

General Procedure for the Preparation of Lariat Ether Methanesulfonates 11−13. To a solution of the lariat ether alcohol (28.9 mmol) and Et_3N (3.21 g, 31.7 mmol) in 500 mL of CH_2Cl_2 was added methanesulfonyl chloride (3.47 g, 30.3 mmol) dropwise at 0 °C. The mixture was stirred at room temperature for 2 h (1 d for **11**), and 100 mL of 5% HCl was added. After 30 min of stirring, the organic layer was separated, washed with saturated aqueous $NaHCO_3$ (2 × 200 mL), brine (100 mL), and water (100 mL), dried ($MgSO_4$), and evaporated in vacuo to give the crude product.

***sym*-(Methanesulfonoxy)dibenzo-14-crown-4 (11):** yield 91% after recrystallization from hexanes−CH_2Cl_2; white solid; mp 183−184 °C; IR 1344, 1251, 1175 cm^{-1}; ^{1}H NMR ($CDCl_3$) δ 2.20−2.50 (m, 2H), 3.19 (s, 3H), 4.20−4.55 (m, 8H), 5.30 (m, 1H), 6.87−7.26 (m, 8H). Anal. Calcd for $C_{19}H_{22}O_7S \cdot 0.1CH_2Cl_2$: C, 56.94; H, 5.55. Found: C, 57.06; H, 5.52. (The presence of CH_2Cl_2 in the analytical sample of **11** was evident in its ^{1}H NMR spectrum.)

***sym*-(Methanesulfonoxy)dibenzo-16-crown-5 (12):** yield 93% after recrystallization from hexanes−CH_2Cl_2; white solid; mp 183−185 °C; IR 1359, 1268, 1175, 1147 cm^{-1}; ^{1}H NMR ($CDCl_3$) δ 3.24 (s, 3H), 3.91−3.96 (m, 4H), 4.15−4.19 (m, 4H),

4.33−4.53 (m, 4H), 5.29 (m, 1H), 6.84−7.02 (m, 8H). Anal. Calcd for $C_{20}H_{24}O_8S$: C, 56.59; H, 5.70. Found: C, 56.52; H, 5.75.

***sym*-(Methanesulfonoxy)dibenzo-19-crown-6 (13):** yield 91% after chromatography through a short alumina column with EtOAc−hexanes (1:1) as eluent; colorless oil; IR 1355, 1258, 1203, 1175, 1125 cm^{-1}; ^1H NMR ($CDCl_3$) δ 3.21 (s, 3H), 3.78 (s, 4H), 3.81−3.91 (m, 4H), 4.13−4.18 (m, 4H), 4.38−4.41 (m, 4H), 5.34 (m, 1H), 6.85−7.04 (m, 8H). Anal. Calcd for $C_{22}H_{28}O_9S$: C, 56.40; H, 6.02. Found: C, 56.38; H, 6.17.

General Procedure for the Synthesis of Lariat Ether Amines 5−7. To a solution of the lariat ether mesylate (1.4 mmol) in dry DMF (20 mL) were added NaN_3 (0.14 g, 2.15 mmol) and Cs_2CO_3 (0.35 g, 1.08 mmol). The mixture was stirred at 105 °C (80 °C for **6**) for 2 d. Most of the DMF was evaporated in vacuo, *but not to dryness because of the instability of organic azides*. The residue was dissolved in 50 mL of CH_2Cl_2, and the solution was washed with H_2O (4 × 30 mL) and brine, dried ($MgSO_4$), and concentrated (*not to dryness*) in vacuo. The crude lariat ether azide was passed through a short column of alumina with CH_2Cl_2 as eluent, and the eluate was carefully concentrated to 5 mL in vacuo. The solution was added to a suspension of $LiAlH_4$ (0.11 g, 2.9 mmol) in dry THF (20 mL) at −78 °C. The mixture was allowed to warm to 0 °C and was stirred at 0−5 °C for 1 h. At 0 °C, H_2O was carefully added to destroy the excess $LiAlH_4$, 1 mL of 5% aqueous NaOH was added, and the mixture was stirred at room temperature for 1 h. The mixture was filtered, and the filtrate was evaporated in vacuo to give the crude product.

***sym*-(Amino)dibenzo-14-crown-4 (5):** yield 77% after recrystallization from CH_2Cl_2−hexanes; white solid; mp 120−122 °C; IR 3372, 1252, 1118 cm^{-1}; ^1H NMR ($CDCl_3$) δ 1.56 (br s, 2H), 2.56−2.30 (m, 2H), 3.50 (m, 1H), 4.11−4.28 (m, 8H), 6.88−7.00 (m, 8H). Anal. Calcd for $C_{18}H_{21}NO_4$: C, 68.55; H, 6.71; N, 4.44. Found: C, 68.51; H, 6.45; N, 4.47.

***sym*-(Amino)dibenzo-16-crown-5 (6):** yield 75% after recrystallization from CH_2Cl_2−hexanes; white solid; mp 123−124 °C; IR 3381, 3311, 1258, 1224, 1122 cm^{-1}; ^1H NMR ($CDCl_3$) δ 2.15 (br s, 2H), 3.55 (m, 1H), 3.92−3.95 (m, 4H), 4.07−4.26(m, 8H), 6.83−7.00 (m, 8H). Anal. Calcd for $C_{19}H_{23}NO_5$: C, 66.07; H, 6.71; N, 4.06. Found: C, 65.79; H, 6.50; N, 4.31.

***sym*-(Amino)dibenzo-19-crown-6 (7):** yield 81% after chromatography on alumina with EtOAc−MeOH (10:1) as eluent; white solid; mp 94−95 °C; IR 3372, 3311, 1257, 1219, 1120 cm^{-1}; ^1H NMR ($CDCl_3$) δ 2.29 (s, 2H), 3.57 (m, 1H), 3.61−3.81 (m, 4H), 3.84−4.00 (m, 6H), 4.13−4.19 (m, 6H), 6.85−7.01 (m, 8H). Anal. Calcd for $C_{21}H_{27}NO_6$: C, 64.77; H, 6.99; N, 3.60. Found: C, 64.47; H, 6.89; N, 3.57.

General Procedure for Preparation of the Anilino-Lariat Ethers 14−25. A mixture of the *sym*-(amino)dibenzocrown ether (4.9 mmol), the appropriate aryl chloride (5.2 mmol), and sodium bicarbonate (0.46 g, 5.5 mmol) in dry MeOH (100 mL) was stirred at room temperature overnight and then refluxed for 1 h. The solvent was evaporated in vacuo, and the residue was dissolved in CH_2Cl_2 (50 mL). The solution was washed with H_2O (2 × 30 mL), dried ($MgSO_4$), and evaporated in vacuo. The residue was chromatographed on silica gel to give the product with CH_2Cl_2−hexanes (1:1) and then CH_2Cl_2 as eluents for the DB14C4 compounds, CH_2Cl_2−hexanes (3:1) and then CH_2Cl_2 as eluents for the DB16C5 compounds, and CH_2Cl_2 and then CH_2Cl_2−EtOAc (10:1) as eluents for the DB19C6 compounds.

***sym*-(2,4,6-Trinitroanilino)dibenzo-14-crown-4 (14):** yield 95%; yellow solid; mp 162−163 °C; IR 3283, 1534, 1330, 1284, 1254, 1118 cm^{-1}; ^1H NMR ($CDCl_3$) δ 2.33−2.40 (m, 2H), 3.88 (m, 1H), 4.14−4.30 (m, 6H), 4.69 (dd, 2H, $^2J_{2A-B}$ = 10.0 Hz, $^3J_{1-2A}$ = 4.4 Hz), 6.81−7.01 (m, 8H), 8.92 (s, 2H), 9.58 (d, 1H, ^3J = 9.4 Hz). Anal. Calcd for $C_{24}H_{22}N_4O_{10}$: C, 54.76; H, 4.21; N, 10.64. Found: C, 54.46; H, 4.27; N, 10.25.

***sym*-(4-Cyano-2,6-dinitroanilino)dibenzo-14-crown-4 (15):** yield 93%; yellow solid; mp 119−121 °C; IR 3297, 2234, 1534, 1352, 1255, 1220, 1118 cm^{-1}; ^1H NMR ($CDCl_3$) δ 2.31−2.38 (m, 2H), 3.82 (m, 1H); 4.12−4.30 (m, 6H); 4.66 (dd, 2H, $^2J_{2A-B}$ = 10.0 Hz, $^3J_{1-2A}$ = 4.3 Hz); 6.78−7.00 (m, 8H); 8.29 (s, 2H); 9.37 (d, 1H, ^3J = 9.5 Hz). Anal. Calcd for $C_{25}H_{22}N_4O_8 \cdot 0.15 CH_2Cl_2$: C, 58.18; H, 4.33; N, 10.79. Found: C, 58.20; H, 4.24; N, 10.46. (The presence of CH_2Cl_2 in the analytical sample of **15** was evident in its ^1H NMR spectrum.)

***sym*-(2,6-Dinitro-4-trifluoromethylanilino)dibenzo-14-crown-4 (16):** yield 90%; yellow solid; mp 147−148 °C; IR 3306, 1541, 1353, 1300, 1256, 1120 cm^{-1}; ^1H NMR ($CDCl_3$) δ 2.31−2.39 (m, 2H), 3.80 (m, 1H), 4.17−4.31 (m, 6H), 4.67 (dd, 2H, $^2J_{2A-B}$ = 9.9 Hz, $^3J_{1-2A}$ = 4.1 Hz), 6.78−7.00 (m, 8H), 8.31 (s, 2H), 9.16 (d, 1H, ^3J = 9.6 Hz). Anal. Calcd for $C_{25}H_{22}F_3N_3O_8$: C, 54.65; H, 4.04; N, 7.65. Found: C, 54.68; H, 3.87; N, 7.47.

***sym*-(2,4-Dinitro-6-trifluoromethylanilino)dibenzo-14-crown-4 (17):** yield 68%; yellow solid; mp 109−110 °C; IR 3416, 3290, 1504, 1338, 1257, 1120 cm^{-1}; ^1H NMR ($CDCl_3$) δ 2.30−2.42 (m, 2H), 4.11−4.35 (m, 7H), 4.62 (dd, 2H, $^2J_{2A-B}$ = 9.2 Hz, $^3J_{1-2A}$ = 3.4 Hz), 6.80−7.00 (m, 8H), 8.45 (br d, 1H, ^3J = 9.0 Hz), 8.65 (d, 1H, ^4J = 2.8 Hz), 9.02 (d, 1H, ^4J = 2.8 Hz). Anal. Calcd for $C_{25}H_{22}F_3N_3O_8$: C, 54.65; H, 4.04; N, 7.65. Found: C, 54.75; H, 3.94; N, 7.50.

***sym*-(2,4,6-Trinitroanilino)dibenzo-16-crown-5 (18):** yield 91%; yellow solid; mp 169−170 °C; IR 3300, 1533, 1330, 1258, 1123, 1063 cm^{-1}. ^1H NMR ($CDCl_3$) δ 3.83−4.27 (m, 11H), 4.54 (dd, 2H, $^2J_{2A-B}$ = 9.7 Hz, $^3J_{1-2A}$ = 5.7 Hz), 6.77−6.94 (m, 8H), 8.99 (s, 2H), 9.52 (d, 1H, ^3J = 10.0 Hz). Anal. Calcd for $C_{25}H_{24}N_4O_{11}$: C, 53.96; H, 4.35; N, 10.07. Found: C, 53.78; H, 4.10; N, 9.84.

***sym*-(4-Cyano-2,6-dinitroanilino)dibenzo-16-crown-5 (19):** yield 88%; yellow solid; mp 208−210 °C; IR 3295, 2233, 1533, 1330, 1258, 1123, 1063 cm^{-1}; ^1H NMR ($CDCl_3$) δ 3.85−4.27 (m, 11H), 4.52 (dd, 2H, $^2J_{2A-B}$ = 9.7 Hz, $^3J_{1-2A}$ = 5.7 Hz), 6.79−6.98 (m, 8H), 8.33 (s, 2H), 9.30 (d, 1H, ^3J = 9.9 Hz). Anal. Calcd for $C_{26}H_{24}N_4O_9$: C, 58.21; H, 4.51; N, 10.44. Found: C, 58.06; H, 4.23; N, 10.05.

***sym*-(2,6-Dinitro-4-trifluoromethylanilino)dibenzo-16-crown-5 (20):** yield 96%; yellow solid; mp 163−164 °C; IR 3320, 1540, 1350, 1261, 1124, 1064 cm^{-1}; ^1H NMR ($CDCl_3$) δ 3.86−4.29 (m, 11H), 4.53 (dd, 2H, $^2J_{2A-B}$ = 9.7 Hz, $^3J_{1-2A}$ = 5.6 Hz), 6.79−6.97 (m, 8H), 8.35 (s, 2H), 9.08 (d, 1H, ^3J = 10.0 Hz). Anal. Calcd for $C_{26}H_{24}F_3N_3O_9$: C, 53.89; H, 4.17; N, 7.25. Found: C, 53.85; H, 4.07; N, 7.05.

***sym*-(2,4-Dinitro-6-trifluoromethylanilino)dibenzo-16-crown-5 (21):** yield 88%; yellow solid; mp 145−147 °C; IR 3418, 3310, 1500,1338, 1260, 1124, 1081 cm^{-1}; ^1H NMR ($CDCl_3$) δ 3.85−4.27 (m, 10H), 4.41 (m, 1H), 4.53 (dd, 2H, $^2J_{2A-B}$ = 9.2 Hz, $^3J_{1-2A}$ = 5.3 Hz), 6.75−6.98 (m, 8H), 8.33 (br d, 1H, ^3J = 7.8 Hz), 8.61 (d, 1H, ^4J = 2.6 Hz), 8.99 (d, 1H, ^4J = 2.6 Hz). Anal. Calcd for $C_{26}H_{24}F_3N_3O_9$: C, 53.89; H, 4.17; N, 7.25. Found: C, 53.86; H, 3.95; N, 6.95.

***sym*-(2,4,6-Trinitroanilino)dibenzo-19-crown-6 (22):** yield 91%; yellow solid; mp 170 °C; IR 3291, 1535, 1330, 1258, 1117 cm^{-1}; ^1H NMR ($CDCl_3$) δ 3.72 (s, 4H), 3.82−3.88 (m, 4H), 4.07−4.16 (m, 5H), 4.32 (dd, 2H, $^2J_{2A-B}$ = 10.3 Hz, $^3J_{1-2B}$ = 4.0 Hz), 4.52 (dd, 2H, $^2J_{2A-B}$ = 10.3 Hz, $^3J_{1-2A}$ = 5.2 Hz), 6.81−7.01 (m, 8H), 8.97 (s, 2H), 9.66 (d, 1H, ^3J = 10.0 Hz). Anal. Calcd for $C_{27}H_{28}N_4O_{12}$: C, 54.00; H, 4.70; N, 9.33. Found: C, 53.64; H, 4.60; N, 9.16.

***sym*-(4-Cyano-2,6-dinitroanilino)dibenzo-19-crown-6 (23):** yield 93%; yellow solid; mp 168−169 °C; IR 3300, 2233, 1534, 1352, 1260, 1120 cm^{-1}; ^1H NMR ($CDCl_3$) δ 3.72 (s, 4H), 3.83−3.87 (m, 4H), 4.02−4.13 (m, 5H), 4.31 (dd, 2H, $^2J_{2A-B}$ = 10.3 Hz, $^3J_{1-2B}$ = 4.0 Hz), 4.49 (dd, 2H, $^2J_{2A-B}$ = 10.3 Hz, $^3J_{1-2A}$ = 5.3 Hz), 6.81−7.03 (m, 8H), 8.33 (s, 2H), 9.44 (d, 1H, ^3J = 9.9 Hz). Anal. Calcd for $C_{28}H_{28}N_4O_{10}$: C, 57.93; N, 4.86; N, 9.65. Found: C, 57.77; N, 4.76; N, 9.49.

***sym*-(2,6-Dinitro-4-trifluoromethylanilino)dibenzo-19-crown-6 (24):** yield 90%; yellow solid; mp 146−147 °C; IR 3314, 1542, 1352, 1304, 1259, 1125 cm^{-1}; ^1H NMR ($CDCl_3$) δ 3.71 (s, 4H), 3.84−3.89 (m, 4H), 3.98 (m, 1H), 4.09−4.13 (m, 4H), 4.34 (dd, 2H, $^2J_{2A-B}$ = 10.3 Hz, $^3J_{1-2B}$ = 4.2 Hz), 4.48 (dd, 2H, $^2J_{2A-B}$ = 10.3 Hz, $^3J_{1-2A}$ = 5.0 Hz), 6.79−7.01 (m, 8H), 8.34 (s, 2H), 9.19 (d, 1H, ^3J = 10.0 Hz). Anal. Calcd for $C_{28}H_{28}F_3N_3O_{10}$: C, 53.94; H, 4.53; N, 6.74. Found: C, 53.72; H, 4.30; N, 6.55.

***sym*-(2,4-Dinitro-6-trifluoromethylanilino)dibenzo-19-crown-6 (25):** yield 88%; yellow solid; mp 136−137 °C; IR

3420, 3300, 1503, 1338, 1264, 1127 cm^{-1}; ^1H NMR ($CDCl_3$) δ 3.76 (m, 4H), 3.84−3.93 (m, 4H), 4.11−4.16 (m, 4H), 4.31−4.40 (m, 3H), 4.42−4.51 (m, 2H), 6.81−7.01 (m, 8H), 8.03 (br s, 1H), 8.61 (d, 1H, ^4J = 2.7 Hz), 8.98 (d, 1H, ^4J = 2.7 Hz). Anal. Calcd for $C_{28}H_{28}F_3N_3O_{10}$: C, 53.94; H, 4.53; N, 6.74. Found: C, 53.77; H, 4.25; N, 6.55.

Preparation of Alkali Metal Salts of Ionized Lariat Ethers 14, 18, and 22 for NMR Investigation. A mixture of the lariat ether in dry THF and an excess of solid alkali metal hydride (LiH, NaH, or KH) was stirred magnetically overnight under nitrogen. During this time, the solution turned from yellow to blood red. The solid was filtered, and the THF was evaporated in vacuo. The residue was dried under high vacuum and then dissolved in dry $CDCl_3$ to give a concentration of approximately 0.02 M.

X-ray Data Collection, Structure Determination, and Refinement. Colorless single crystals of **17**−**19** obtained by slow air evaporation of the lariat ether solutions in CH_2Cl_2−hexanes were mounted on fibers and transferred to the goniometer of a Siemens CCD area detector-equipped platform diffractometer. The crystals were cooled to −100 °C during data collection using a stream of cold nitrogen gas. Data collection, reduction, absorption correction, and structure solution and refinement were carried out with the Siemens software products SMART, SAINT, SADABS, and SHELXTL, respectively. Unit cell data were determined by a global refinment of several thousand reflections within the data collection range. The space groups were determined using systematic absences (or lack thereof) and subsequent solution and successful refinement of the structure (to distinguish between centric and acentric choices). Refinement was full-matrix, least-squares of F^2.

Acknowledgment. This research was supported by the Division of Chemical Sciences of the Office of Basic Energy Sciences of the US Department of Energy (Grant DE-FG03-94ER14416).

Supporting Information Available: Tables of the crystallographic parameters, atomic coordinates and equivalent displacement parameters, torsion angles, bond length and angles, anisotropic displacement parameters, and hydrogen coordinates and isotropic displacement parameters for **17**−**19**. This material is available free of charge via the Internet at http://pubs.acs.org.

JO990116H